AIAA JOURNAL
Vol. 36, No. 3, March 1998

Experimental Study of Causes of Unsteadiness of Shock-Induced Turbulent Separation

Ö. H. Ünalmis* and D. S. Dolling†
University of Texas at Austin, Austin, Texas 78712

Simultaneous measurements have been made of the fluctuating wall pressures under the unsteady separation shock wave in a Mach 5 blunt fin-induced interaction and fluctuating pitot pressures from a triple-tipped probe placed well upstream in the undisturbed turbulent boundary layer. Results show a correlation between the scale of the separated flow and spanwise variations in pitot pressure in the incoming boundary layer. The low-frequency spanwise pitot pressure variations are consistent with earlier experiments, indicating the presence of a spanwise vortex structure in the incoming boundary layer. The results suggest that these vortices may be the cause, or at least one of the causes, of the low-frequency pulsation of the separated flow.

Nomenclature

B	= frequency bandwidth
C_f	= skin-friction coefficient
D	= leading-edge diameter of blunt fin
F_s	= sampling frequency
f	= frequency
$G(f)$	= power spectral density function, $(\text{psia})^2/\text{Hz}$
H	= boundary-layer shape factor
h	= pitot probe height above wall
M	= Mach number
$P, \bar{P}$	= instantaneous and mean pressure
$R[\,]$	= cross-correlation coefficient
Re	= Reynolds number
T	= temperature
t	= time
U	= local mean velocity
U_c	= convection velocity
X	= streamwise coordinate or distance from the leading edge of the blunt fin
Y	= vertical coordinate
Z	= spanwise coordinate
γ	= shock foot intermittency
ΔX	= streamwise separation
ΔY	= vertical separation
ΔZ	= spanwise separation
δ_0	= boundary-layer velocity thickness, $0.99U_\infty$
δ^*	= boundary-layer displacement thickness
θ	= boundary-layer momentum thickness
λ	= spanwise spacing between vortex pairs
ξ	= smallest separation between transducers, 0.115 in.
Π	= wake strength
ρ	= density
σ_{Pw}, σ_{Pt}	= standard deviation of wall and pitot pressure signals
τ	= time delay

Subscripts

e/a	= ensemble averaged
o	= undisturbed flow
t	= evaluated at pitot probe tip
w	= evaluated at wall
0	= stagnation condition
∞	= freestream condition

Received Feb. 28, 1997; revision received Sept. 29, 1997; accepted for publication Oct. 25, 1997.

*Postdoctoral Fellow, Center for Aeromechanics Research, Department of Aerospace Engineering and Engineering Mechanics. Member AIAA.

†Professor, Center for Aeromechanics Research, Department of Aerospace Engineering and Engineering Mechanics. Associate Fellow AIAA.

Introduction

IN computations of shock-wave/turbulent-boundary-layer interaction, there are often significant discrepancies between the predictions and the measurements, particularly when large-scale separation occurs. It is not likely that the discrepancies are due entirely to numerical problems or insufficiently fine meshes but most likely are the result of inadequate turbulence modeling and the neglect of experimentally observed flowfield unsteadiness. In many interactive flows, unsteadiness is important because many design criteria, such as maximum permissible structural loading and fatigue life, are controlled by the fluctuating pressure loads and intermittent heating.

Although interactive flows have been studied extensively for several decades, much of the earlier research only provided information about mean surface properties and flowfield structure. During the last decade, more attention has been paid to flowfield unsteadiness. A relatively recent review of interaction unsteadiness has been compiled by Dolling.[1] Experimental work[2–6] has shown that the separation shock foot motion and hence the expansion/contraction (or pulsation) of the separated flow in an unswept compression ramp interaction has two primary components: low-frequency, large-scale motion and high-frequency, small-scale motion. Figure 1 shows an example of the separation shock foot history in a piecewise continuous form for a 28-deg unswept compression ramp flow at Mach 5. This was deduced from the analysis of eight simultaneously sampled wall pressure signals. The analysis technique[4,7] is based on a boxcar representation of the intermittent surface pressure signals. With a small spacing between transducers, the shock foot position can be bracketed quite accurately. As can be seen from Fig. 1b, the low- and high-frequency motions of the separation shock are superposed on each other, and there is no clear demarcation between them.

Erengil and Dolling[5] examined separation shock foot unsteadiness in different two-dimensional and three-dimensional interactions and concluded that the separation shock unsteadiness can be attributed to two different physical phenomena. 1) The small-scale motion of the separation shock is caused by its response to fluctuations in the ratio of static quantities across the shock foot induced by passage through the shock of turbulent structures in the incoming boundary layer. 2) The large-scale motion of the separation shock is caused by its displacement due to the expansion and contraction motion of the separated flow.

However, item 2) is simply an observation and does not explain why the separation bubble undergoes this low-frequency, large-scale expansion/contraction motion. A reasonable question is whether some low-frequency activity in the boundary layer induces the expansion/contraction motion of the bubble. Some evidence in support of that idea comes from the work of McClure.[6] He used the same 28-deg unswept compression ramp model under the same flow conditions as was used in Ref. 5. In one of his experiments the signal from a small, high-frequency response pitot probe mounted

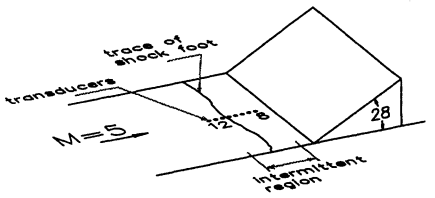

a) Schematic of experiment

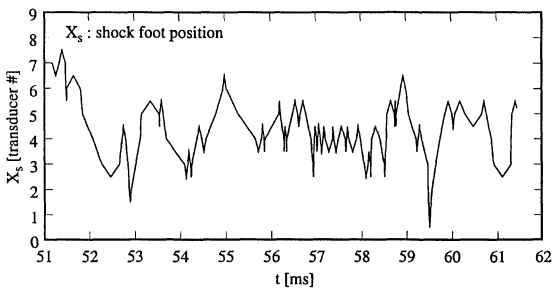

b) Shock foot history (from Ref. 1)

Fig. 1 Sample shock foot history in a Mach 5 compression ramp interaction.

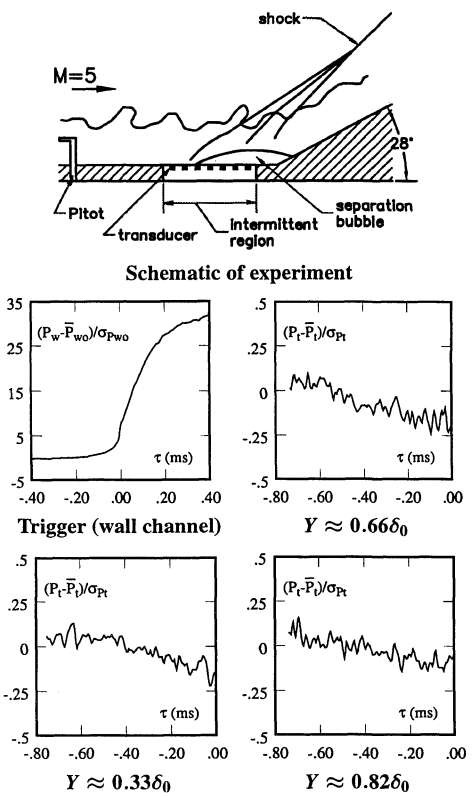

Fig. 2 Ensemble-averaged pitot pressure for an upstream shock sweep (pressure histories from Ref. 6).

far upstream ($\approx 16\delta_0$) of the compression corner was recorded simultaneously with wall pressure signals under the separation shock. Ensemble-averaged pitot pressure histories were then calculated for upstream and downstream sweeps of the separation shock (Fig. 2). For pitot probe heights less than about $0.9\delta_0$, there was a gradual decrease in pitot pressure during an upstream shock motion and a gradual increase during a downstream shock motion. The timescale of the shock motions and the corresponding rises and falls in pitot pressure were on the order of 1 ms. During such a time interval the freestream flow travels almost 1 m, and assuming large-scale turbulent structures have a streamwise length scale of order δ_0, 20–40 such structures pass by a fixed point in the interaction. Because there exists a long duration variation in pitot pressure with certain shock foot motions, it may be inferred that the boundary layer has a low-frequency behavior that is connected to the shock and the bubble motion.

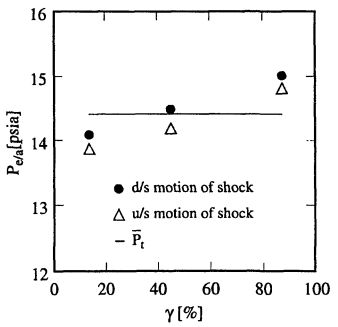

Fig. 3 Ensemble-averaged pitot pressure as a function of intermittency.

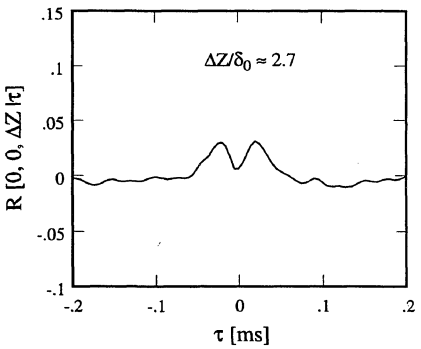

Fig. 4 Example of spanwise correlation with unexpected features.

A different analysis of McClure's data by the current authors (Fig. 3) shows that when the separation bubble is at its maximum size, the average pitot pressure in the upstream boundary layer at a fixed height above the wall is lower than the mean pitot pressure and the opposite is true when the bubble is at its minimum size.[8] Low intermittency (where intermittency is defined as the percentage of time that the separation shock foot is upstream of a given point) corresponds to the shock foot far forward. The fact that the ensemble-averaged pitot pressure has different values for the two extreme scales of the separation bubble initially suggested a simplistic model involving a low-frequency thickening/thinning motion of the boundary layer. When the boundary layer thickens, the fixed pitot probe would read a lower value because its effective height in the boundary layer decreases. The opposite would be true for a thinning motion of the boundary layer. However, more recent work using planar laser scattering and particle image velocimetry in the same flowfield suggests that the overall boundary-layer thickness does not vary with separated flow scale but that there may be systematic variations in the lower part of the boundary-layer velocity profile.[9]

Earlier work by Marshall and Dolling[10] in compression ramp interactions had shown that the spanwise rippling of the shock foot remained coherent over a distance of order $2\delta_0$, which is not consistent with spanwise scales of turbulent structures in supersonic turbulent boundary layers.[11] If the shock foot motion is driven directly by the incoming flow itself, then this anomaly raises the question of what in the incoming flow has a spanwise scale of order $2\delta_0$. Alternatively, is there an instability in the separated flow (perhaps triggered by the incoming flow) that controls the spanwise scale of the shock foot dynamics?

Measurements by the first author[12] have shown the existence of a spanwise vortex structure in the boundary layer used in the earlier experiments. The investigation that led to this conclusion was triggered by the unusual behavior of the cross-correlation coefficient at certain spanwise separations of wall pressure transducers (Fig. 4). The cross-correlation coefficient at this spanwise separation of $2.7\delta_0$ exhibits a twin peak. If only large-scale turbulent structures were present, a single maximum at zero time delay would be seen. Further, results from another experiment in which the spanwise separation of two transducers was fixed and the pair was shifted systematically across the tunnel showed a periodic variation of cross-correlation maximum (Fig. 5). The spanwise scale of the periodicity is about $2\delta_0$. To demonstrate that such a variation was due to a naturally occurring vortex structure, experiments were carried out (Fig. 6a) using vortex generators of different types placed upstream of the

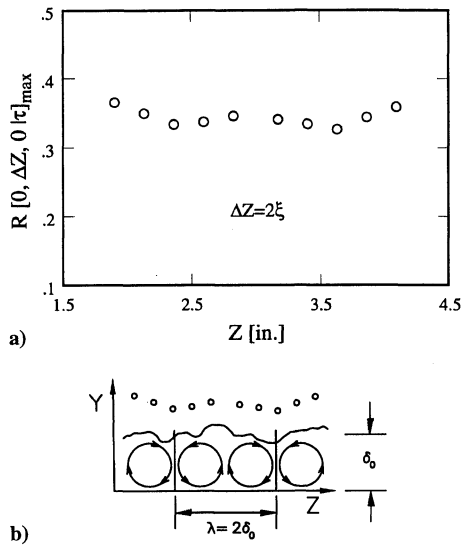

Fig. 5 a) Variation of maximum cross-correlation coefficient across tunnel floor span and b) hypothetical vortex system.

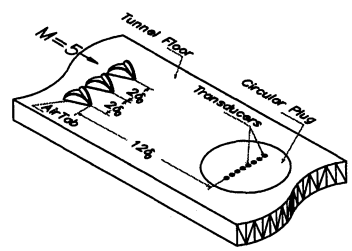

a) Schematic of experiment (not to scale)

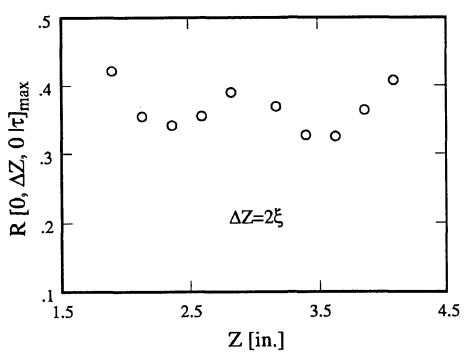

b) Variation of maximum cross-correlation coefficient

Fig. 6 Variation of maximum cross-correlation coefficient across tunnel floor span in the presence of AirTabs™ (1ξ = 0.115 in. $\approx 0.19\delta_0$, smallest separation between transducers).

transducer array. It was shown that a deliberately created vortex pattern causes a similar variation in the cross-correlation maximum (Fig. 6b).

It is evident that some of the most fundamental issues related to the unsteadiness of shock-induced separated flows still need clarification. Although the proposed cause of the high-frequency, small-scale motion of the shock foot seems physically reasonable, the cause of the large-scale unsteadiness of the separation bubble, which is of primary concern in modeling and engineering applications, is not yet clear. It appears that the boundary layer has a low-frequency component, although the origin of this component is yet to be understood. A key question is whether this low-frequency behavior is a naturally occurring feature of a supersonic turbulent boundary layer or is a wind-tunnel phenomenon that is tunnel specific. Note that it is not unique to the Mach 5 blowdown tunnel used in the current experiment because the unsteadiness just described is seen in a wide variety of continuous and blowdown tunnels. This is an important question because the existing experimental data sets that are used to validate computations consist of mean surface and flowfield data that are time averages of the unsteady properties. Should the character of the unsteadiness be a function of the facility, the time-averaged properties of a given interaction may also be facility dependent.

The primary objective of the current work is to examine the relation between the low-frequency behavior of the boundary layer and the separated flow. This has been done through simultaneous measurements of fluctuating wall pressure in the intermittent region ahead of a blunt fin (to monitor the expansion/contraction of the separated flow) and fluctuating pitot pressures from a triple-tipped pitot probe placed in the boundary layer well upstream of the interaction region.

Experimental Program

Wind Tunnel and Flow Conditions

All of the experiments were conducted in the Mach 5 blowdown tunnel of the University of Texas at Austin. The constant-area test section is 6 in. (15.2 cm) wide by 7 in. (17.8 cm) high and has a length of 12 in. (30.5 cm). Removable side doors allow access to an instrumented floor section. A total of about 140 ft^3 (4 m^3) of compressed air is provided by a Worthington HB4 four-stage compressor and stored in external tanks at a pressure of about 2500 psia (17.24 MPa). Two 420-kW banks of nichrome wire resistive heaters located upstream of the stagnation chamber heat the incoming air to the desired stagnation temperature, which is measured by a Type J thermocouple. These heaters can provide stagnation temperatures of up to 759°R (422 K). The stagnation pressure and temperature for the present experiments were 325 psia (2.24 MPa ± 1%) and 640°R (356 K ± 1%), respectively. With these stagnation conditions, stable run times of up to 1 min could be obtained. The freestream Mach number was 4.95, the freestream velocity was 2520 ft/s (768 m/s), and the unit Reynolds number was 14.6×10^6/ft (48×10^6/m).

The incoming boundary layer undergoes natural transition and develops under approximately adiabatic wall temperature conditions. The boundary-layer thickness δ_0 is based on the height in the boundary layer where the mean velocity reaches 99% of the freestream value, unless specified otherwise. Measured values of basic parameters of the undisturbed turbulent boundary layer on tunnel centerline approximately 2.6 in. (6.6 cm) upstream of the ramp corner line are given in Table 1.

A hemicylindrically blunted fin of 0.75 in. (1.91 cm) leading-edge diameter was used to generate the separated flow.[13] The fin is 4 in. (10.16 cm $\approx 6.7\delta_0$) high. It has a 1.0-in. (2.54-cm)-wide base extension that fits into a slot in the floor with screws underneath securing it in place. With the aid of 0.0576-in. (0.146-cm)-long gauge blocks, the distance between the fin leading edge and intermittent region transducers could be set accurately.

Instrumentation

Fluctuating wall pressure measurements were made using Kulite Semiconductor Products, Inc., Model XCQ-062-15A and XCQ-062-50A transducers. These transducers have a nominal outer diameter of 0.0625 in. (0.159 cm) and a pressure-sensitive diaphragm of 0.028 in. (0.071 cm) in diameter. Perforated screens above the diaphragm protect the transducer from damage due to any dust particles in the flow but limit the frequency response of both models to about 50 kHz. This bandwidth is more than sufficient to capture the separation shock frequencies, which have been shown to be about 0.3–2.0 kHz for unswept and 2–7 kHz for swept flows.[1] The characteristic frequency of the larger boundary-layer structures, on the other hand, is expected to be on the order of $U_0/(1-2\delta_0)$, which corresponds to a frequency of 25–50 kHz. The transducers

Table 1 Incoming boundary-layer properties

Parameter	Value
δ_0, 0.99 U_∞	0.59 in. (1.50 cm)
δ_0, 0.99 $(\rho U)_\infty$	0.70 in. (1.78 cm)
δ^*	0.26 in. (0.66 cm)
$H \equiv \delta^*/\theta$	10.2
Π	0.78
Re_θ	2.97×10^4
$C_f(\times 10^4)$	7.74

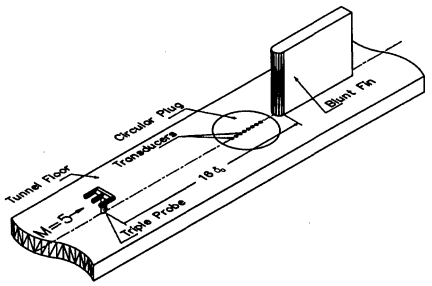

Fig. 7 Triple-tipped pitot probe upstream of a blunt fin (not to scale).

were installed in a circular brass plug mounted flush with the tunnel floor. Transducers could be flush mounted along four different rows on this plug. The first and mostly used row has 26 ports, whereas the second, third, and fourth rows have 8, 13, and 12 ports, respectively. Because the distance between consecutive ports ξ is 0.115 in. (0.292 cm $\approx 0.2\delta_0$), a maximum separation of 2.875 in. (7.303 cm $\approx 4.8\delta_0$) could be obtained on the primary row.

Fluctuating pitot pressure measurements were made using a triple-tipped probe in which three Kulite miniature pressure transducers (XCQ-062-100A) were installed. Each transducer is mounted in a tapered stainless steel tube with the tip protruding 0.05 in. (0.13 cm) upstream of the tube opening. The spanwise separation between the centers of transducers is 0.3 in. (0.76 cm), about one-half boundary-layer thickness ($\delta_0 \approx 0.6$ in. $= 1.52$ cm). Overall, the three tips span one boundary-layer thickness.

Data Acquisition

Output from the Kulite pressure transducers was amplified by either Dynamics (Model 7525), Vishay Measurements Group (Model 2311), or PARC (Model 113) amplifiers. The amplified signals were then filtered using Ithaco (Models 4113 or 4213) analog filters. The filter cutoff for broadband measurements was set at 50 kHz, although most of the tests were made at lower settings because the focus in the blunt fin-induced interaction tests was on the low-frequency content of the signal. For the broadband measurements a sampling rate of 200 kHz was chosen to capture more events over a longer time duration. For the low-pass tests the signal was analog filtered at 20 and 5 kHz for 50- and 20-kHz sampling frequencies, respectively. The filter settings were chosen as the next available settings below the Nyquist frequency to avoid aliasing. The signal-to-noise ratio was about 100 in most cases but overall ranged from 50 to 150.

Data were acquired using two LeCroy analog-to-digital (A/D) converters with 12-bit resolution (Model 6810 waveform recorders). Each A/D converter has four megabytes of memory and can sample one channel of data at rates up to 5 MHz or four channels of data simultaneously at rates up to 1 MHz per channel. The two A/Ds can acquire data from eight channels simultaneously when triggered using the same clock. Usually either 256 or 512 records of data per channel were acquired. All data analysis was performed on a Hewlett–Packard 9000 Series 380 computer.

Test Program

Using the experimental arrangement in Fig. 7, simultaneous fluctuating wall pressure and pitot pressure measurements were made. The triple-tipped pitot probe was placed about $16\delta_0$ upstream of the blunt fin. The wall transducers in the intermittent region were placed at 2.83, 2.72, 2.49, 2.26, and 2.03 in. (7.2, 6.9, 6.3, 5.7, and 5.14 cm, respectively) upstream of the blunt fin. Because of concerns that the probe would interfere with the interaction, comparisons were first made between the mean and the root mean square pressures, the intermittency profiles, and intermittent region power spectra for both the probe-in and probe-out cases. Later, the triple-tipped probe was used alone to examine the behavior of the boundary-layer pitot signal in different bandwidths.

Analysis Techniques

Conditional data analysis methods as well as standard time series analysis were used. The most important elements of the conditional data analysis technique are the event, its definition, and its detection. The event is based on the physics of the problem (in this case, a shock passage over a transducer) and is detected by means of threshold values, which are set by the user. If the signal value exceeds a threshold value, or some combination of thresholds, then an event occurs.

The variable-window ensemble-averaging technique[4] was used to analyze the data. The term variable-window refers to the width of the data window of any particular shock passage. The width of the window for any given shock passage depends on both the preceding and following shock passages. For example, if a given upstream shock passage is assigned the number 2, then the preceding and following shock passages would be numbers 1 and 3, respectively. The data window then extends from the middle of 1 and 2 to the middle of 2 and 3. Because the duration of these passages will be different, the window size will vary; hence the name. For the details of this technique the reader is referred to Ref. 4. The choice of the threshold settings was based on a sensitivity analysis by Dolling and Brusniak.[7]

Discussion of Results

Effects of Pitot Probe on the Interaction Region

The primary concern in using a probe upstream of any separated flow is the possible interference on the interaction. The pitot probe used in McClure's[6] experiments was a single-tip, streamlined, floor-mounted probe that had a support with a diamond cross section. McClure reported an upstream shift in the interaction from its undisturbed position ranging from 0.17 to $0.83\delta_0$, depending on probe height. Measurements made by Gramann and Dolling[14] showed that this increase in interaction size did not affect the shock dynamics significantly, and subsequent surface pressure measurements showed that the interference effects decreased rapidly spanwise.

The triple probe used in this investigation also had a diamond cross-section floor support and was larger than the single probe used by McClure. The expectation was that it would result in more extensive interference. However, examination of the signals from the intermittent region transducers shows that the compression ramp interaction is far more sensitive to perturbations to the incoming boundary layer than is the blunt fin interaction. The effects of the triple probe on the intermittent region are summarized in Fig. 8. The mean pressure (Fig. 8a), the rms of the wall pressure fluctuations (Fig. 8b), and the shock foot intermittency γ (Fig. 8c) are plotted vs X/D. Data from the two most upstream wall transducers for probe-in and probe-out cases show the same mean and standard deviations of about 0.6 and 0.014 psia, respectively (Figs. 8a and 8b). The

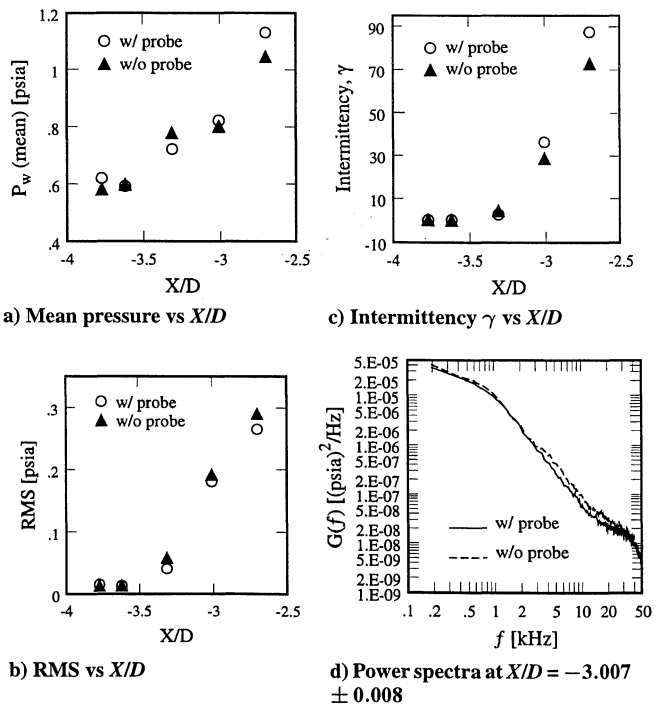

a) Mean pressure vs *X/D*

c) Intermittency γ vs *X/D*

b) RMS vs *X/D*

d) Power spectra at *X/D* = −3.007 ± 0.008

Fig. 8 Effects of triple probe on the intermittent region.

intermittency is zero in both cases (Fig. 8c). The effects of the interaction are first seen on the third upstream transducer. The mean pressure, standard deviation, and intermittency have slightly higher values in both cases compared with the undisturbed values of upstream transducers (Fig. 8), showing that with and without the probe in the test section the onset of the interaction region did not change much. The two most downstream channels also exhibit very close values of mean, standard deviation, and intermittency in both cases. Their high values compared with those from the upstream transducers clearly indicate frequent shock passages over the downstream transducers. The power spectra with and without the probe are also plotted for one location ($X/D = -3.007 \pm 0.008$) in Fig. 8d and are also in good agreement particularly at frequencies typical of the shock motion (<3–4 kHz).

In summary, measurements with and without the probe in place show that the triple probe does not have a significant effect on the location of the intermittent region, the shock strength, or the shock dynamics.

Results of Variable-Window Ensemble-Averaging Analysis

Ensemble-averaged pitot pressure histories for each tip of the triple-tipped probe and for the triggering channel in the intermittent region for an upstream motion of the shock foot are given in Fig. 9. The probe tip is at $Y = 0.4 \pm 0.016$ in. (1.02 cm $\approx 0.67\delta_0$), the analog filter cutoff is 12.5 kHz, and the sampling frequency is 50 kHz. Tips 1 and 3 (Figs. 9a and 9c, respectively) are the side tips, and tip 2 (Fig. 9b) is the center tip. Two cases are shown. The dashed lines correspond to a small-scale separated flow. The triggering channel (Fig. 9d) in this case is a wall pressure transducer that is located 2.03 in. (5.14 cm $\approx 2.7D$) upstream of the blunt fin. At this location the signal is about 92% intermittent (i.e., the separation shock foot is essentially at its farthest downstream position). For this case the number of ensembles is 1629. The sharp increase in pressure around zero time delay in Fig. 9d (dashed line) shows that the shock is crossing the triggering channel in the upstream direction. Examination of the corresponding pitot channels (dashed lines) shows that 1) the pressure on tip 1 (the side tip) is close to the mean and for negative τ is rising, 2) the pressure on tip 2 (the center tip) is substantially above the mean value (about 6% at $\tau \approx -0.3$ ms) and decreasing, and 3) the pressure on tip 3 (the other side tip) is below its mean (about 3% at $\tau \approx -0.3$ ms) and rising. An identical analysis using the same data and with the same trigger channel, but for a downstream motion of the shock, gave the same results.

However, when the trigger is a channel with low intermittency (about 4%), the ensemble-averaged pitot pressure shows trends opposite to those seen for high intermittency (solid lines in plots). The triggering channel in this case is located 2.49 in. (6.3 cm $\approx 3.3D$) upstream of the blunt fin, and the number of ensembles is 927. Examination of the solid lines in Fig. 9 shows that 1) the pressure on tip 1 is now below the mean and relatively constant, 2) the pressure on the center tip is substantially below the mean (about 8% at $\tau \approx -0.3$ ms compared with 6% above the mean when the shock foot is downstream) and now rising (rather than falling) for negative time delays, and 3) the pressure on tip 3 is now about 3% above its mean at $\tau \approx -0.3$ ms and falling (rather than 3% below and rising as in the dashed line in Fig. 9c). An identical analysis using the same data sets, the same trigger channel but for a downstream shock motion, gave the same results.

To assess the significance of the preceding results the same data were reanalyzed. The only difference was that the ensemble averaging of the pitot pressure signals was not triggered by shock passages but essentially on a random basis (Fig. 10). The approach was the following: the 256 records of data (corresponding to the small separated flow) were divided into 1629 equal segments (the number 1629 corresponds to the number of ensembles used in Fig. 9). Then a window of arbitrary size was chosen (100 points in this case) and placed at the beginning of each segment, and the corresponding pitot signals were ensemble averaged. Figures 10a–10c show that the pitot pressures are now close to their mean values and do not show any systematic rises or falls as they did when shock passages were used as the trigger.

When the transducer signals were sampled at 20 kHz (and analog filtered at 5 kHz), a larger number of ensembles could be obtained due to a longer data-taking time. The pitot probe height was the same ($Y = 0.4 \pm 0.016$ in. $= 1.02$ cm $\approx 0.67\delta_0$). Figures 11a–11c show ensemble-averaged pitot pressure histories for different shock foot motions (upstream and downstream) and positions (shock foot far upstream or far downstream). Figure 11d shows the pressure histories of the two corresponding triggering wall transducers. In all cases the solid line is for the large separated flow, and the dashed

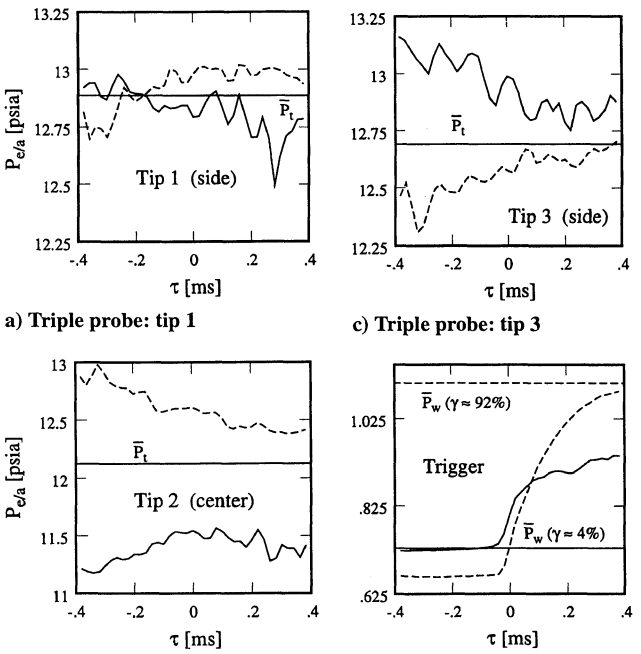

Fig. 9 Ensemble-averaged pressure histories for an upstream motion of shock foot ($h = 0.4 \pm 0.016$ in. $\approx 0.67\delta_0$, $\Delta Z = 0.3 \pm 0.016$ in. $\approx 0.5\delta_0$, $F_s = 50$ kHz, and $B = 0$–12.5 kHz); ——, large separated flow (shock foot is upstream) and – – –, small separated flow (shock foot is downstream).

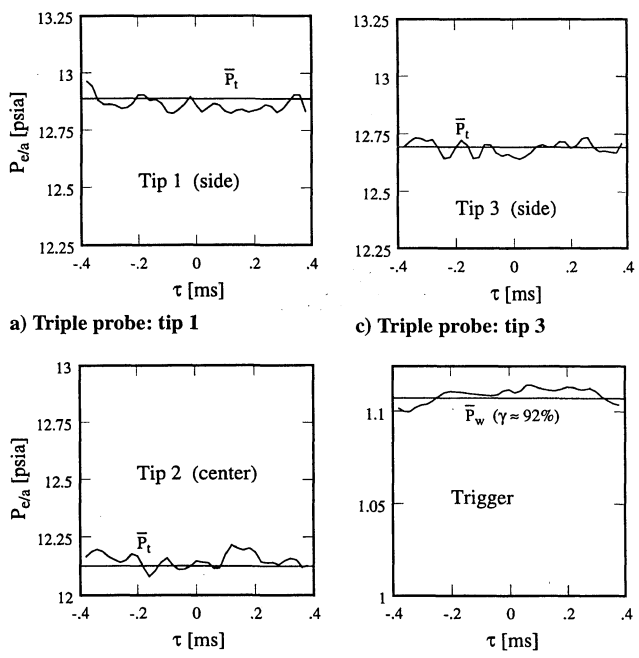

Fig. 10 Ensemble-averaged pressure histories for random signal on a triggering channel with high intermittency (upstream motion of shock foot) ($h = 0.4 \pm 0.016$ in. $\approx 0.67\delta_0$, $\Delta Z = 0.3 \pm 0.016$ in. $\approx 0.5\delta_0$, $F_s = 50$ kHz, and $B = 0$–12.5 kHz).

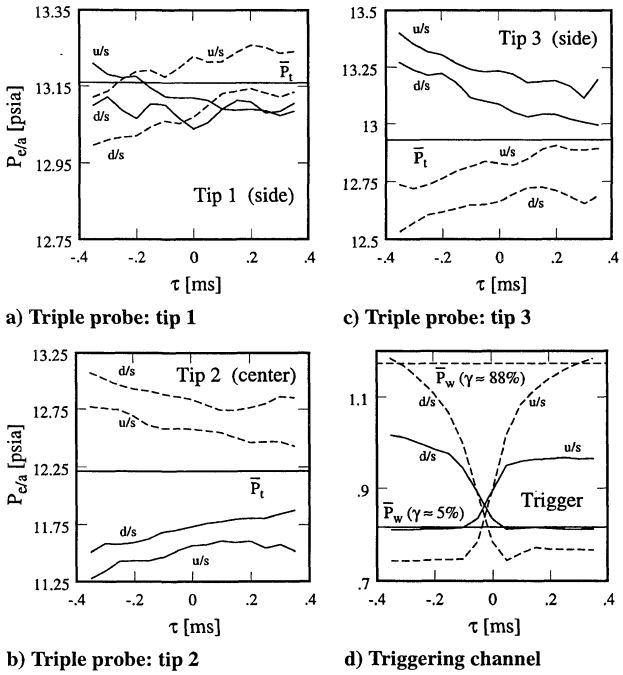

Fig. 11 Ensemble-averaged pressure histories for certain positions and motions of shock foot ($h = 0.4 \pm 0.016$ in. $\approx 0.67\delta_0$, $\Delta Z = 0.3 \pm 0.016$ in. $\approx 0.5\delta_0$, $F_s = 20$ kHz, and $B = 0$–5 kHz); ——, large separated flow (shock foot is upstream); – – –, small separated flow (shock foot is downstream); *u/s*, upstream motion of shock foot; and *d/s*, downstream motion of shock foot.

line is for the small separated flow. The number of ensembles for the large separated flow is 2091, and the intermittency at the location of the triggering wall transducer is about 5%. In the case of the small separated flow, the number of ensembles is 4120, and the intermittency is about 88%. Comparison of Figs. 11b and 11c shows that for the center tip of the probe (tip 2) and for the side tip (tip 3) the behaviors of the ensemble-averaged pitot pressure histories have exactly opposite trends: in the case of the center tip, for the small separated flow, the pressure is above the mean value and decreasing irrespective of the direction of the shock foot motion, whereas in the case of the large separated flow, the pressure is below the mean and rising with increasing τ, again irrespective of the direction of the shock foot motion. On the other hand, on the side tip (tip 3), the pitot pressure is above the mean and decreasing for the large separated flow and vice versa for the small separated flow. Examination of Fig. 11a shows that although the trends of the ensemble-averaged pressure history on tip 1 are not as clear as for the other two tips, closer inspection shows that they are consistent with the ones observed on the other side tip (especially for the small separated flow).

Earlier it was mentioned that analysis of McClure's compression ramp data by the current authors showed that when the separation bubble is at its maximum size, the average pitot pressure in the upstream boundary layer at a fixed height above the wall is lower than the mean pitot pressure and the opposite is true when the bubble is at its minimum size. In that analysis, the results of which are given in Fig. 3, there was a time delay between the ensemble in the intermittent region and that in the incoming boundary layer. This time delay was calculated from the distance between the probe location and the triggering transducer using an appropriate convection velocity (90% of the freestream velocity). However, when a time delay was not used, identical results were obtained. These are not shown here, but simply by inspection of Figs. 2 and 11 (for the compression ramp and blunt-fin cases, respectively) it can be seen that a time delay of about 0.3 ms will not alter the result. This independence of a time delay suggests that the relation between the boundary-layer pitot pressure and the shock foot position does not depend on individual events that convect downstream (such as large-scale turbulent structures) but rather depends on the global behavior of the flow.

Comparisons of Figs. 11a–11c show that the trends seen in the ensemble-averaged pitot pressure histories are independent of the

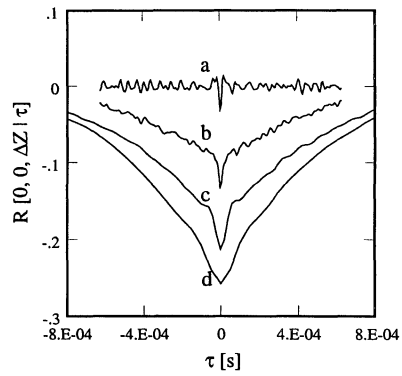

Fig. 12 Sample cross correlations for different bandwidths (triple-tipped pitot probe, tips 1 and 2; $h = 0.4 \pm 0.016$ in. $\approx 0.66\delta_0$ and $\Delta Z = 0.3 \pm 0.016$ in. $\approx 0.5\delta_0$): a) $F_s = 200$ kHz and $B = 12.5$–50 kHz, b) $F_s = 200$ kHz and $B = 0$–50 kHz, c) $F_s = 50$ kHz and $B = 0$–12.5 kHz, and d) $F_s = 20$ kHz and $B = 0$–5 kHz.

direction of the shock foot motion but closely correlated with the extreme positions of the shock foot. Hence there is a clear correlation between the scale of the separated flow and pitot pressure levels in the incoming boundary layer.

Boundary-Layer Measurements

Experiments at various sampling rates using the triple probe were also made in the tunnel floor boundary layer. From the ensemble-averaging analysis presented earlier, the results of which are shown in Fig. 11, it was seen that when the pitot pressure on one tip is below the mean, the pressure on an adjacent tip is above the mean. If such behavior was an underlying systematic feature of the continuous pitot signals, then it might be expected that the cross correlation would be negative. Figure 12 shows cross correlations of the signals from tips 1 and 2 for different bandwidths. Recall that the tips have a spanwise separation of 0.3 in. (0.76 cm $\approx 0.5\delta_0$). In this case the tips are 0.4 in. (1.02 cm $\approx 0.67\delta_0$) above the tunnel floor. In the broadband case (0–50 kHz, curve b), the correlation is negative with a sharp but small peak value of about −0.14. The magnitude is small because of the small number of turbulent structures whose spanwise scales are equal to or greater than $0.5\delta_0$. This is evident from the narrow-band results (12.5–50 kHz) shown as curve a. In this case, the correlation is essentially zero at all τ except very close to zero where a small, but noticeable, peak occurs. Curves c and d are low-pass-filtered correlations at 0–12.5 and 0–5 kHz, respectively. To acquire sufficient data, the sampling rates were reduced in these cases to 50 (curve c) and 20 kHz (curve d). With decreasing low-frequency bandwidth, the correlation curves become broader, and the peak increases in magnitude. The sharp peak due to turbulence clearly visible in curves a, b, and c is less obvious in curve d when the upper value of the frequency band is reduced to 5 kHz. These results show that there exists a low-frequency component in the incoming boundary layer below the frequency range in which large-scale turbulent structures might be expected to exist. The negative peak is consistent with the results obtained earlier using ensemble averaging. Moreover, because the correlation exists for spanwise separations beyond the typical length scale of turbulent structures, this is further support for the view that there is an underlying global structure as well as a local one, i.e., turbulence.

Low-pass-filtered (0–12.5 kHz) cross correlations of the signals from tips 1 and 2, 2 and 3, and 1 and 3 are shown in Fig. 13. The probe is 0.3 ± 0.016 in. (0.76 cm $\approx 0.5\delta_0$) above the tunnel floor, and the sampling rate is 50 kHz. The correlation for tips 1 and 2 (curve b) is, as expected, essentially the same as curve c of Fig. 12. The peak correlation magnitude is slightly higher, indicating that the spanwise turbulence scales are slightly larger closer to the wall. Curve a, the cross correlation between tips 1 and 3, does not show a significant peak. This is, initially, a little surprising because if vortices, such as those shown in Fig. 5b, are present, one might expect that a negative correlation would be observed between probe tips spaced apart $1\delta_0$ spanwise. The reason is that on one edge of the vortex the boundary layer is thicker, leading to a lower pitot pressure, whereas on the

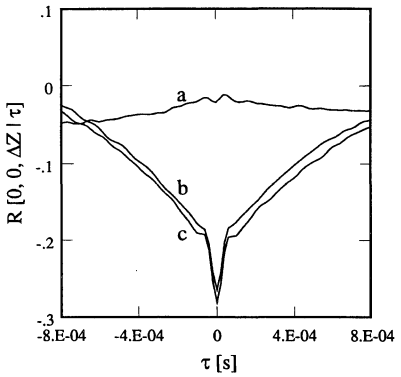

Fig. 13 Sample cross correlations for spanwise separations (triple-tipped pitot probe, $h = 0.3 \pm 0.016$ in. $\approx 0.5\delta_0$, $F_s = 50$ kHz, and $B = 0$–12.5 kHz): a) $\Delta Z = 0.6$ in. (tips 1 and 3), b) $\Delta Z = 0.3$ in. (tips 1 and 2), and c) $\Delta Z = 0.3$ in. (tips 2 and 3).

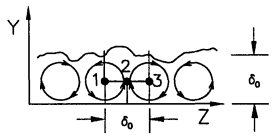

Fig. 14 Front view of the triple-tipped pitot probe in the boundary layer combined with a hypothetical vortex system.

other edge it is thinner, leading to a higher pitot pressure. However, one cannot be certain of the position of the naturally developing vortex structure with respect to the probe tips in this case. Figure 14 shows the front view of the triple probe experiments combined with a hypothetical vortex system. The center tip, tip 2, of the probe is on the centerline of the tunnel floor. If it is assumed that the hypothetical vortex system in Fig. 14 is representative of the actual picture, then tip 1 is at the core of one vortex structure, whereas tip 3 is at the core of a neighboring structure. Tip 2 would then be in the upwash region. The mean pitot pressure values at the locations of tips 1 and 3 should be very close to each other, whereas tip 2 would have a lower mean value. The measurements confirm this: Tips 1 and 3 have mean pressure values higher than those of tip 2 in all the experiments performed. From a cross-correlation perspective, one can argue that there is always going to be a relative pressure variation in opposite direction between the center tip (tip 2) and the side tips. The reason is that the pressure reading on the center tip will consistently be lower (for an upwash region, or higher for a downwash region) than the ones on the side tips. This is the reason for the negative cross correlation between the side tips and the center tip in Fig. 13. On the other hand the same argument cannot be made for the side tips, and if, as shown in Fig. 14, both the probe and vortex structure are symmetric about the tunnel centerline, the pressure signals will not result in any significant correlation, as is indeed the case for curve a of Fig. 13.

Overall, although there are clearly systematic variations in spanwise pitot pressure that result in a negative correlation coefficient, the correlation is relatively weak. Doubtlessly the underlying behavior responsible does not occur all of the time, and even when it does, it may well be partly masked by turbulence.

Discussion

In the absence of unambiguous visual evidence or detailed three-dimensional, time-dependent flowfield maps, which are virtually impossible to obtain, it is difficult to develop a watertight physical model. Although the available data appear consistent and would seem to support the following ideas, such a model should be viewed as a challenge for future experiments (or computations) to examine further.

Before the current study some experiments provided strong evidence of an underlying (weak) spanwise vortical structure in the undisturbed boundary layer. The present triple-tipped probe measurements are consistent with such a conclusion. Cross correlations at spanwise spacings beyond that characteristic of large-scale turbulent structures show evidence of a low-frequency component that produces negative correlation coefficients. Such a negative correlation is generated by one probe signal being above its mean while the other is below its mean. The magnitude of the peak correlation increases as the bandwidth is decreased to the range characteristic of the expansion/contraction of the separated flow. The facts that a correlation exists at low frequencies, is relatively broad, and occurs at large (relative to turbulent length scales) spanwise spacing suggest that the cause may well be the underlying vortical structure in the boundary layer.

Ensemble averaging showed that these spanwise rises and falls in pitot pressure in the incoming flow correlate with the scale of the separated flow. This leads to the inference that these boundary-layer vortices may be the cause (or at least one cause) of the unsteadiness of the separated flow. The boundary layer has both large-scale turbulent structures as well as an underlying (weak) vortical structure. In a continuous flow there will be times when the relative dominance of one component is larger than the other and at that time plays the larger role. Planar laser Mie scattering[15] has shown that there are times when the boundary layer is relatively quiescent and others when there exists a long train of large-scale structures, indicating that significant structural changes are possible. Thus it is probable that the shock foot behavior is the result of both systematic changes in incoming boundary conditions induced by the underlying vortical structure together with changes in boundary conditions induced by passage of large-scale structures.

Summary

Simultaneous measurements have been made of the fluctuating wall pressures under the unsteady separation shock wave in a blunt fin-induced interaction and fluctuating pitot pressures from a triple-tipped probe placed well upstream in the undisturbed turbulent boundary layer. The experiments were performed in a Mach 5 blow-down tunnel. Results show a correlation between the scale of the separated flow and spanwise variations in pitot pressure in the incoming boundary layer. The spanwise variations in pitot pressure at low frequency are consistent with earlier experiments, indicating the presence of a spanwise vortex structure in the incoming boundary layer. These vortices may be the cause, or at least one of the causes, of the low-frequency pulsation of the separated flow. The origin of these vortices is not clear and would take a very sophisticated experimental program to determine. In fact, the problem might be better addressed via computational fluid dynamics.

Acknowledgments

Support for this research has been provided through grants from the Army Research Office (DAAL03-91-G-0023) monitored by T. Doligalski and from NASA Langley Research Center (NAG1-1471) monitored by W. E. Zorumski. These sources of support are gratefully acknowledged.

References

[1]Dolling, D. S., "Fluctuating Loads in Shock Wave/Turbulent Boundary Layer: Tutorial and Update," AIAA Paper 93-0284, Jan. 1993.

[2]Gramann, R. A., and Dolling, D. S., "Dynamics of Separation and Reattachment in a Mach 5 Unswept Compression Ramp Flow," AIAA Paper 90-0380, Jan. 1990.

[3]Erengil, M. E., and Dolling, D. S., "Correlation of Separation Shock Motion with Pressure Fluctuations in the Incoming Boundary Layer," *AIAA Journal*, Vol. 29, No. 11, 1991, pp. 1868–1877.

[4]Erengil, M. E., and Dolling, D. S., "Unsteady Wave Structure near Separation in a Mach 5 Compression Ramp Interaction," *AIAA Journal*, Vol. 29, No. 5, 1991, pp. 728–735.

[5]Erengil, M. E., and Dolling, D. S., "Physical Causes of Separation Shock Unsteadiness in Shock Wave/Turbulent Boundary-Layer Interactions," AIAA Paper 93-3134, July 1993.

[6]McClure, W. B., "An Experimental Study of the Driving Mechanism and Control of the Unsteady Shock Induced Turbulent Separation in a Mach 5 Compression Corner Flow," Ph.D. Dissertation, Dept. of Aerospace Engineering and Engineering Mechanics, Univ. of Texas, Austin, TX, Aug. 1992.

[7]Dolling, D. S., and Brusniak, L., "Separation Shock Motion in Fin, Cylinder, and Compression Ramp Induced Turbulent Interactions," *AIAA Journal*, Vol. 27, No. 6, 1989, pp. 734–742.

[8]Ünalmis, Ö. H., and Dolling, D. S., "Decay of Wall Pressure Field and Structure of a Mach 5 Adiabatic Turbulent Boundary Layer," AIAA Paper 94-2363, June 1994.

[9]Beresh, S. J., Clemens, N. T., Dolling, D. S., and Comninos, M. C., "Investigation of the Causes of Large Scale Unsteadiness of Shock-Induced Separated Flow Using Planar Laser Imaging," AIAA Paper 97-0064, Jan. 1997.

[10]Marshall, T. A., and Dolling, D. S., "Spanwise Properties of the Unsteady Separation Shock in a Mach 5 Unswept Compression Ramp Interaction," *AIAA Journal*, Vol. 30, No. 8, 1992, pp. 2056–2065.

[11]Spina, E. F., "Organized Structures in a Supersonic Turbulent Boundary Layer," Ph.D. Dissertation, Dept. of Mechanical and Aerospace Engineering, Princeton Univ., Princeton, NJ, Oct. 1988.

[12]Ünalmis, Ö. H., "Structure of the Supersonic Turbulent Boundary Layer and Its Influence on Unsteady Separation," Ph.D. Dissertation, Dept. of Aerospace Engineering and Engineering Mechanics, Univ. of Texas, Austin, TX, Aug. 1995.

[13]Brusniak, L., "Physics of Unsteady Blunt Fin-Induced Shock Wave/Turbulent Boundary Layer Interactions," Ph.D. Dissertation, Dept. of Aerospace Engineering and Engineering Mechanics, Univ. of Texas, Austin, TX, May 1994.

[14]Gramann, R. A., and Dolling, D. S., "A Preliminary Study of Turbulent Structures Associated with Unsteady Separation Shock Motion in a Mach 5 Compression Ramp Interaction," AIAA Paper 92-0744, Jan. 1992.

[15]Chan, S. C., Clemens, N. T., and Dolling, D. S., "Flowfield Imaging of Unsteady, Separated Compression Ramp Interactions," AIAA Paper 95-2195, June 1995.

R. W. Wlezien
Associate Editor